

## Single-electron tunneling effects in a metallic double dot device

T. Junno,<sup>a)</sup> S. -B. Carlsson,<sup>b)</sup> H. Q. Xu, and L. Samuelson<sup>c)</sup>

*Solid State Physics/The Nanometer Consortium, Lund University, Box 118, S-221 00 Lund, Sweden*

A. O. Orlov and G. L. Snider

*Department of Electrical Engineering, University of Notre Dame, Notre Dame, Indiana 46556*

(Received 29 May 2001; accepted for publication 13 November 2001)

We report on differential conductance measurements on a gold double-dot structure at 4.2 K. The two dots were connected in series by tunnel junctions formed by atomic force microscopy manipulation of nanodisks. The tunnel junctions were made strongly asymmetric. The characteristic honeycomb-shaped charging diagram separating different Coulomb blockade regions of well-defined occupancy of electrons was observed and the cells in the charging diagram were found to be skewed by the asymmetry of the tunnel junctions. In addition, a double-dot Coulomb staircase structure, with steps of varying width, was observed and was studied for varying gate voltage. The occupancy of electrons on the two dots was determined as a function of both drain source and gate voltages. © 2002 American Institute of Physics. [DOI: 10.1063/1.1436532]

Recently, much attention has been brought to the possibility of using the Coulomb interaction between single electrons, residing on coupled quantum dots, as a basis for device architecture. One example is quantum-dot cellular automata (QCA),<sup>1,2</sup> in which arrays of coupled quantum dots are used to implement various logic functions.<sup>3–6</sup> The smallest building block of QCA is a cell of two coupled dots, a double dot, with one excess electron occupying either of the dots.<sup>5</sup> By changing the charge configuration on a nearby cell or on control gates close to the double dot, a switching between stable states, representing “0” or “1” can be generated and digital data can be transmitted and manipulated. Until now, however, studies of coupled-dot devices were done for semiconductor dots or metal-oxide Dolan-bridge junctions.<sup>7,8</sup>

Here, we present a study of a gold double-dot structure, fabricated using mechanical tuning of tunnel junctions<sup>9</sup> by atomic force microscopy (AFM). With this technique dot capacitance,  $C$ , of the order of 10 aF and charging energy,  $e^2/2C$ , of about 80 meV can be achieved. Thus, the effects of the Coulomb blockade in the device can be well observed at temperature above the liquid nitrogen temperature. For convenience, our investigation of the double-dot device was carried out at 4.2 K (the liquid helium temperature). In the fabrication, the tunnel junctions were made strongly asymmetric, and the effects of asymmetric junctions were studied in both the zero-bias conductance and the current–voltage ( $I$ – $V$ ) curves. The asymmetry was found to skew the characteristic honeycomb-shaped cells in the charging diagram and to give a distinct Coulomb staircase, with steps of varying width, in the  $I$ – $V$  curves.

Figure 1 shows a schematic picture of our device with an equivalent circuit diagram. It consists of two Au dots  $D_1$  and

$D_2$  in series connected by tunnel junctions and capacitively coupled to two gate electrodes. Each dot is composed of two  $\sim 60$  nm wide Au disks in mechanical contact with each other, one of which can be moved by AFM manipulation while the other is fixed by a thin titanium layer between the disk and the substrate, acting as an adhesive. The electrodes and the fixed disks were fabricated on an oxidized silicon substrate by electron beam lithography and evaporation of 5 nm Ti and 30 nm Au. Additional 30 nm thick *movable* Au disks were placed in a grid pattern close to the fixed disks by a second lithography and evaporation step. The tunnel junctions were produced by AFM manipulation,<sup>9</sup> by reducing the initially  $\sim 50$  nm wide gaps separating the source and drain electrodes and the fixed disks to a width of a couple of ångströms using three movable disks [see Fig. 1(a)]. The tunnel resistances were tuned so that  $R_3 \gg R_2 \gg R_1$ . After fabrication

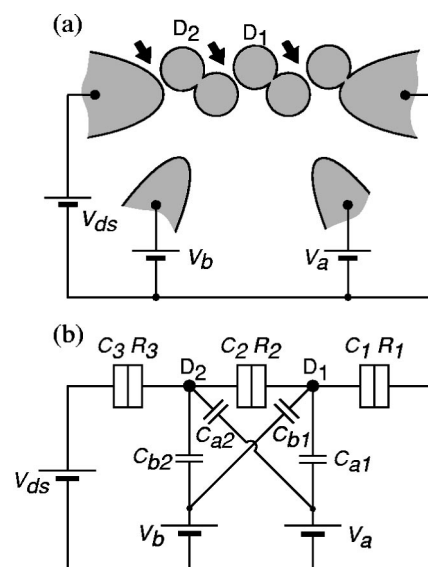


FIG. 1. (a) Schematic image of the double-dot device. Each of the dots, denoted  $D_1$  and  $D_2$ , consists of two 60 nm Au disks in contact with each other. The three tunnel junctions are indicated by arrows; (b) circuit diagram of the device in (a).

<sup>a)</sup>Present address: Ericsson Mobile Communications AB, Scheelevägen 15, S-221 83 Lund, Sweden.

<sup>b)</sup>Present address: Accenture, Sveavägen 25, Box 1331, S-111 83 Stockholm, Sweden.

<sup>c)</sup>Author to whom correspondence should be addressed; electronic mail: lars.samuelson@ftf.lth.se

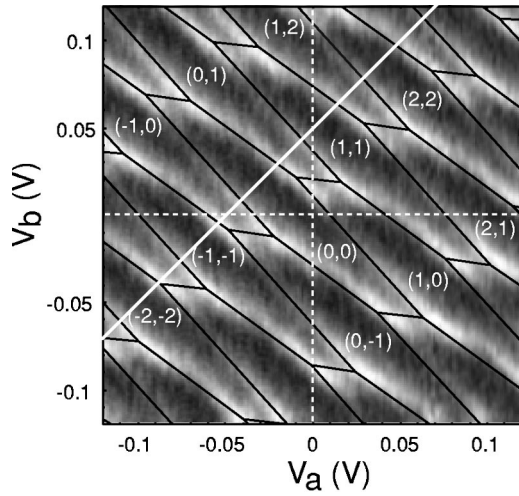


FIG. 2. Conductance of the double-dot system as function of gate voltages,  $V_a$  and  $V_b$ , with a theoretical fit [Eq. (1)] to the charging diagram. Bright regions correspond to high conductance. The numbers of excess electrons on the dots are indicated as  $(n_1, n_2)$ .

the device was cooled to 4.2 K in a liquid helium dewar. The total resistance at 4.2 K was 1.6 G $\Omega$ .

Conductance of the double dot was measured using standard lock-in technique with an ac excitation of 0.5 mV at frequencies of 5–20 Hz. Figure 2 shows the zero-bias conductance as a function of the gate voltages  $V_a$  and  $V_b$ , together with calculated Coulomb blockade regions using  $C_1 = 16.9$ ,  $C_2 = 13$ ,  $C_3 = 6.5$ ,  $C_{a1} = 2.6$ ,  $C_{a2} = 1.6$ ,  $C_{b1} = 1.8$ , and  $C_{b2} = 3.1$  aF. Points of high conductance constitute the corners, triple points, of hexagonal blockade regions or cells in a honeycomb pattern.<sup>10</sup> Within each cell the number of excess electrons on the two dots  $(n_1, n_2)$  is constant. The theoretical fit was done by calculating the electrostatic charging energy of the two dots from the equation:

$$E_C(n_1, n_2) = \sum_i \frac{1}{2} Q_i(n_1, n_2) V_i(n_1, n_2), \quad (1)$$

where the sum goes over all the electrodes and islands in Fig. 1(a), under the assumption that the charge in each of the dots is quantized as  $n_1 e$  and  $n_2 e$ , and the assumption that  $n_1 = 0$  and  $n_2 = 0$  when all the applied voltage to the electrodes  $V_i = 0$ , i.e., assuming that there are no charges in the dots when no voltages are applied to all the electrodes. For a given set of applied voltages  $V_i$ , the charges  $Q_i$  of the electrodes and the numbers of excess electrons in the dots,  $n_1$  and  $n_2$ , can be determined using Kirchhoff's law for various loops in the circuit. Regions of well-defined occupancy  $(n_1, n_2)$  are separated by lines where  $E_C(n_1, n_2) = E_C(n_1 + 1, n_2)$ ,  $E_C(n_1, n_2) = E_C(n_1, n_2 + 1)$ , or  $E_C(n_1, n_2) = E_C(n_1 + 1, n_2 - 1)$ . Here we note that although the initial configuration of the charge,  $n_1 = 0$  and  $n_2 = 0$ , when all the voltages applied to the electrodes  $V_i = 0$  were assumed, the actual, initial distribution of the charges in the double-dot system can be different in different measurements, due to, e.g., change in the configuration of the background charges in the substrate. Thus, the charge occupancy  $(n_1, n_2)$  determined for Fig. 2 is the configuration of the numbers of excess electrons, in the two dots, induced by the voltages applied to the gates.

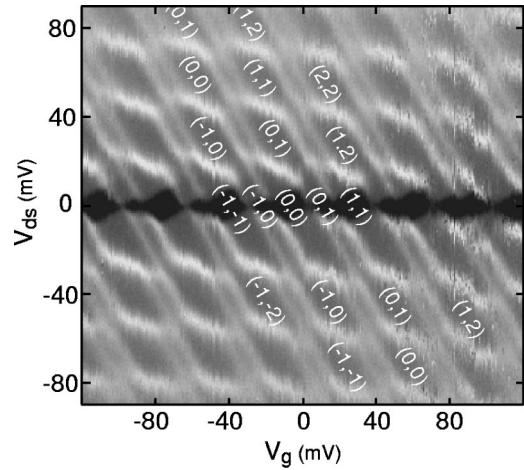


FIG. 3. Conductance of the double-dot system as function of drain-source voltage  $V_{ds}$  and gate voltage  $V_g$ . Regions of constant excess charge are separated by bright lines corresponding to high differential conductance.

The shape of the periodic cell is determined by all the capacitances involved. Ideally, each gate should couple only to its corresponding dot. However, in the present device geometry there is a considerable cross coupling between a dot and the gate belonging to the other dot, i.e., the capacitances  $C_{a2}$  and  $C_{b1}$  in Fig. 1. Figure 2 shows that by sweeping gate voltage  $V_a$  while keeping  $V_b = 0$  (as indicated by the horizontal dashed line in Fig. 2), or by sweeping gate voltage  $V_b$  while keeping  $V_a = 0$  (as indicated by the vertical dashed line in Fig. 2), we are able to change the numbers of electrons in the two dots alternately. Also, cross coupling results in a diagonal stretching of the cell, as manifested in Fig. 2. Furthermore, due to strong asymmetry in the capacitances,  $C_1$  and  $C_3$ , of the tunnel junctions, the honeycomb cells are skewed so that the shorter connecting lines between the nearest neighboring triple points have an angle to the  $V_a$  axis differing significantly from 45 degrees (i.e., the case for the device with symmetric tunnel junctions,  $C_1 = C_3$ ).

We also measured the double dot differential conductance,  $dI/dV$ , as a function of drain-source voltage,  $V_{ds}$ , and gate voltage,  $V_g$ , with  $V_g$  applied to both gates, i.e.,  $V_a = V_b = V_g$  (Fig. 3). Small and large diamond-shaped Coulomb blockade regions alternate with the gate voltage  $V_g$ . The small diamond gradually grows in size with increasing gate voltage  $V_g$ , while the large diamond decreases. The width of the diamonds at  $V_{ds} = 0$  is the same as the width of the hexagonal cell in Fig. 2, marked by the white solid line. Note that in ideal case, the width of the diamonds at  $V_{ds} = 0$  would be related to the width of the hexagonal cell, following the  $V_a = V_b$  line in Fig. 2. The shift in the gate voltages at  $V_{ds} = 0$  from this ideal case, seen in Fig. 3, is due to the fact that the initial charge distributions of the double-dot system are different in the two measurements. From the zero-bias blockade regions marked with the white solid line in Fig. 2 the occupation of excess electrons  $(n_1, n_2)$  for each blockade region at  $V_{ds} = 0$  in Fig. 3 can be identified.

Similar to the case of an asymmetrically coupled single dot, lines of high differential conductance, corresponding to steps in the I–V curve, are observed when the number of excess electrons on the two dots changes by one. However, in contrast to the single-dot device where only one slope is

found and the steps are equidistant, two different slopes are present, resulting in steps of varying width. Steps of variable width have been observed in granular metal films using a scanning tunneling microscope,<sup>11</sup> and were explained by assuming a double-dot structure. Our measurements confirm this and, in addition, display the gate dependence of the steps.

In an asymmetrically coupled *single-dot* device, the tunnel rates at some applied  $V_{ds}$  for an electron to enter or to leave the dot are different from each other. Therefore, when  $V_{ds}$  is increased, the number of excess electrons on the dot either increases or decreases, in steps, depending on which of the two tunnel resistances is larger. This gives rise to a Coulomb staircase in the I–V characteristics. For a *double-dot* system, the behavior of  $n_1$  and  $n_2$  as a function of  $V_{ds}$  depends on which of the three resistances  $R_1$ ,  $R_2$ , and  $R_3$  is the largest. If  $R_1$  is dominant,  $n_1$  and  $n_2$  both decrease with increasing  $V_{ds}$ . If  $R_2$  is the largest,  $n_1$  increases while  $n_2$  decreases, whereas, if  $R_3$  is dominant, as in our case,  $n_1$  and  $n_2$  both increase with increasing  $V_{ds}$ . Thus, we can identify the occupancy of excess electrons on the two dots as a function of  $V_{ds}$  as well (see Fig. 3).

In conclusion, we have presented conductance measurements at 4.2 K on a gold double-dot device fabricated by AFM manipulation of nanodisks. The tunnel junctions were made strongly asymmetric, and the effects of asymmetric junctions were studied in both the zero-bias conductance and the current–voltage (I–V) curves. The asymmetry was found to skew the characteristic honeycomb-shaped cells in the charging diagram and to result in a distinct Coulomb stair-

case, with steps of varying width, in the I–V curves. It was also observed that at zero bias the numbers of excess electrons on the two dots could be controlled by applying voltages to capacitively coupled gate electrodes, while at finite bias the numbers of excess electrons on the two dots were controlled by the gate voltages as well as the drain–source voltage. Our double-dot structure may, when coupled together in pairs, be used to investigate critical parameters for the realization of QCA architecture at high temperatures.

This research was supported in part by NFR, TFR, NUTEK, SSF, and the ESPRIT Charge Program as well as by the Office of Naval Research.

<sup>1</sup>C. S. Lent, P. D. Tougaw, W. Porod, and G. H. Bernstein, *Nanotechnology* **4**, 49 (1993).

<sup>2</sup>C. S. Lent and P. D. Tougaw, *J. Appl. Phys.* **74**, 6227 (1993).

<sup>3</sup>A. O. Orlov, I. Amlani, G. H. Bernstein, C. S. Lent, and G. L. Snider, *Science* **277**, 928 (1997).

<sup>4</sup>I. Amlani, A. O. Orlov, G. L. Snider, C. S. Lent, and G. H. Bernstein, *Appl. Phys. Lett.* **71**, 1730 (1997).

<sup>5</sup>A. O. Orlov, I. Amlani, G. Toth, C. S. Lent, G. H. Bernstein, and G. L. Snider, *Appl. Phys. Lett.* **74**, 2875 (1999).

<sup>6</sup>I. Amlani, A. O. Orlov, G. Toth, G. H. Bernstein, C. S. Lent, and G. L. Snider, *Science* **284**, 289 (1999).

<sup>7</sup>G. J. Dolan, *Appl. Phys. Lett.* **31**, 337 (1997).

<sup>8</sup>T. A. Fulton and G. J. Dolan, *Phys. Rev. Lett.* **59**, 109 (1987).

<sup>9</sup>S.-B. Carlsson, T. Junno, L. Montelius, and L. Samuelson, *Appl. Phys. Lett.* **75**, 1461 (1999).

<sup>10</sup>H. Pothier, P. Lafarge, C. Urbina, D. Esteve, and M. H. Devoret, *Europhys. Lett.* **17**, 249 (1992).

<sup>11</sup>E. Bar-Sadeh, Y. Goldstein, C. Zhang, H. Deng, B. Abeles, and O. Millo, *Phys. Rev. B* **50**, 8961 (1994).